INTERNATIONAL JOURNAL OF HYDROGEN ENERGY 48 (2023) 16769–16778

Available online at www.sciencedirect.com

ScienceDirect

journal homepage: www.elsevier.com/locate/he

Superconducting state of the van der Waals layered PdH_2 structure at high pressure

Prutthipong Tsuppayakorn-aek [a,b,1], *Arnab Majumdar* [c,1], *Rajeev Ahuja* [c,d], *Thiti Bovornratanaraks* [a,b], *Wei Luo* [c,*]

[a] *Extreme Conditions Physics Research Laboratory and Center of Excellence in Physics of Energy Materials (CE:PEM), Department of Physics, Faculty of Science, Chulalongkorn University, Bangkok 10330, Thailand*

[b] *Thailand Center of Excellence in Physics, Ministry of Higher Education, Science, Research and Innovation, 328 Si Ayutthaya Road, Bangkok 10400, Thailand*

[c] *Condensed Matter Theory Group, Materials Theory Division, Department of Physics and Astronomy, Uppsala University, Box 516, SE-751 20, Uppsala, Sweden*

[d] *Department of Physics, Indian Institute of Technology Ropar, Rupnagar 140001, Punjab, India*

HIGHLIGHTS

- PdH_2 has a superconducting transition temperature of 24 K at ambient pressure.
- The crystalline to vdW layered structural transition occurs at 15 GPa.
- The abnormal high-T_c at high pressure is associated with the out-of-plane interlayer breathing vibrational mode in our model.

ARTICLE INFO

Article history:
Received 21 March 2022
Received in revised form
19 December 2022
Accepted 26 December 2022
Available online 1 February 2023

ABSTRACT

We report structural and superconducting transitions in layered van der Waals (vdW) palladium dihydride (PdH_2) calculated under high-pressure compression. PdH_2 has a Hexagonal Closed-Packed (HCP) structure with a space group of $P6_3mc$, and has a superconducting transition temperature of 24 K at ambient pressure. At 15 GPa, the crystalline to vdW layered structural transition occurs, while the superconductivity remains. On compressing from 15 to 50 GPa, the T_c increased abnormally by 3.5 K. It is found that the superconducting critical temperature of $P6_3mc$ PdH_2 is determined by the out-of-plane interlayer breathing vibrational mode. As a vdW layered metal hydride superconductor, PdH_2 provides a platform to study hydride superconductivity in such kinds of materials.

Introduction

The crystallography of hydrogen–rich materials at high pressure is interesting as they hold the promise to be room temperature superconductors. In 1968, British solid-state physicist Ashcroft made his earlier prediction of high critical temperature (T_c) superconductivity in high-pressure metallic hydrogen [1], he further proposed that the presence of heavier main group elements in hydrides besides hydrogen can significantly increase the electron phonon coupling [2]. This is because the

* *Corresponding author.*
E-mail address: wei.luo@physics.uu.se (W. Luo).
[1] These coauthors contributed equally to this work.

https://doi.org/10.1016/j.ijhydene.2022.12.312

heavier elements reduce the physical pressure required for metallization via chemical pre-compression. These predictions, based on the Bardeen-Cooper-Schrieffer (BCS) theory [3] of phonon mediated superconductivity led the way to extensive research (both experimental and theoretical) on high pressure hydrides for the search for high T_c superconductors [4–14]. Using *ab initio* calculations, several hydrogen rich compounds have been proposed to be high T_c conventional superconductors, whose critical temperatures are calculated to be very high [15–23]. Recently, experimentalists found superconductivity above 260 K in lanthanum superhydride at megabar pressure [24]. With regards to the study of superconducting properties of the hydrides, it is imperative to know their crystal structures. Besides, the various structural morphologies, for example clathrate, modulated, etc., there have been experimental works which have reported that hydrogen–rich materials like xenon hydrides can exist at high pressures owing to van der Waals (vdW) forces [25,26]. The vdW force is important at both ambient and high pressure, which is reported in the theoretical study that mentions the fine balance between vdW forces and hydrogen bonding in ambient and high–pressure phases of ice [27]. In an exemplary work by Strobel et al., the Raman and Infrared (IR) spectra were found to have unique features of the vdW forces that play an important role in the high pressure interactions of silane and hydrogen [28]. Similarly, another class of hydrides is garnering interest of late. These are the layered hydride materials, with van der Waals interactions, which also show potential superconducting properties. One such material that we have proposed in this work is PdH_2.

The superconductivity of the Pd–H system is dependent on the hydrogen concentration. In general PdH_x has superconducting potential and the critical temperature increases with the increase of H atom concentration [29]. For the H:Pd ratio of 0.81, a $T_c = 1.3$ K was observed. At a highest concentration ratio of about 1.0, the T_c to the superconducting state was found to be higher than 8.0 K [30]. So basically, PdH_x phase is a superconducting state, with T_c about 1–9 K for x close to 1 [29,31]. The remarkable experimental observation indicated that the ratio of hydrogen to palladium in Pd–H systems can be continuously increased by increasing the H concentrations. Recently, Syed et al. [32] have observed the superconductivity of PdH_x, with x approaching 1, by measuring the resistance of the sample. The experimental observation revealed that PdH has a T_c of 54 K. Therefore, extrapolating the idea further, PdH_2 might also undergo metallization and eventually become a superconductor on being compressed. Calculations have pointed out that the face-centered cubic (FCC) structure of PdH_2 is unstable under compression. Structural prediction simulations reveal that the PdH_2 phase should exist in the hexagonal closed–packed structure with space group $P6_3mc$ [33]. Furthermore, it has been predicted to exist as a mono–layered structure by the *ab initio* random structure searching (AIRSS) technique [34,35]. The effect of pressure displays the electronic structure evolution of the mono–layered structure, which shows the transition from the metallic state to the semi–metallic state in the PdH_2. Generally, compounds bonded with van der Waals (vdw) forces tend to be good candidates for 2D superconductors [36,37]. This is due to their saturated cleavage plane and flexible physical and chemical properties. Besides the carrier densities, even the electron–phonon coupling, electron–electron interactions and other physical parameters, can be modulated upon doping, intercalation, *etc.* In this letter, we have used *ab initio* lattice dynamics calculations to account for the dynamical stability of the predicted $P6_3mc$ PdH_2 structure. We have explored the layered structure of PdH_2, which is seen to undergo a single layered to vdW–layered transition as a function of pressure as two non-interacting layers come closer on being compressed and start to interact. The T_c of the vdW–layered structure has also been investigated under high pressure. We have discussed the possible impact of the van Hove singularity and occurrence of interlayer breathing mode on the calculated superconducting properties.

Computational details

The structural optimizations and total energy calculations were performed at 0, 15, 20, 30, 40, 50 and 60 GPa using both VASP [38,39] and Quantum ESPRESSO [40]. For both the codes, the projector augmented wave (PAW) method [41,42], and the generalized gradient approximation (GGA) with the Perdew-Burke-Ernzerhof parametrization (PBE) [43] have been used to describe the electronic exchange-correlation effects. The results from both the codes are consistent. A dense Monkhorst-Pack [44] k-point mesh (12 × 12 x 6) was used for the Brillouin zone integration for the optimization of the structures. We have studied the lattice dynamics and vibrational properties of monolayered PdH_2 using the supercell approach, as implemented in the VASP code [38,39] and the Phonopy package [45,46]. The calculations were conducted employing 2 × 2 x 2 supercells, consisting of 48 atoms, for the $P6_3mc$-layered structure by using a plane-wave basis-set energy cut-off of 700 eV. Since, the layers interact at higher pressures, the dispersion corrections of the form $C^6.R^{-6}$ are treated by the semi-empirical DFT-D2 vdW corrections [47]. For the $P6_3mc$ PdH2 vdW–layered structures, we calculated the electron phonon coupling (EPC) with density functional perturbation theory using Quantum Espresso [40]. A plane-wave energy cut-off of 60 Ry is used. The EPC matrix elements were computed in the first BZ with 4 × 4 x 2 q-meshes while the individual EPC matrices were obtained with a 24 × 24 x 12 k-points mesh.

Results

Crystal structure

Similar to other studies concerning layered structures [48,49], intriguing structural properties are seen for our predicted PdH_2 system as well. In another related work of ours, we have reported a layered hexagonal structural phase of PdH_2 having a space group of $P6_3mc$ obtained from *ab-initio* structural prediction method [33]. The structural morphology at ambient pressure comprises of layers of PdH_2 (Fig. 1). It is clear that this layered structure consists of hydrogen atoms occupying two distinct Wyckoff positions. We have classified them as H_{2a} and H_{2b} for convenience. The H_{2a} atoms are bonded to the Pd atoms with a bond length of 1.877 Å at ambient pressure,

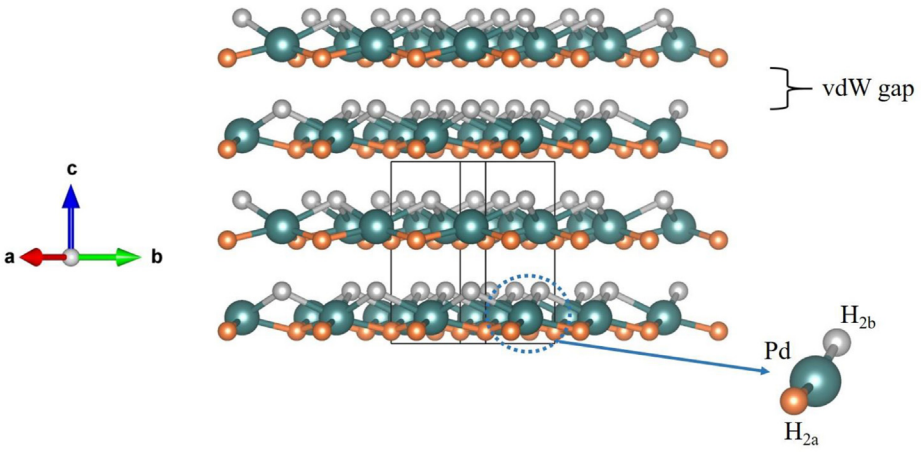

Fig. 1 – Schematic illustration of the $P6_3mc$ PdH_2 vdW layered structure. The Pd atoms are shown in dark green, the H_{2a} atoms in orange, and the H_{2b} atoms in grey colour. (For interpretation of the references to color in this figure legend, the reader is referred to the Web version of this article.)

forming extended monolayers. The distance between the H_{2b} and their coordinated Pd atoms at 0 GPa is 1.873 Å, while the same hydrogen atoms (H_{2b}) are at a distance of 3.30 Å from the nearest Pd atoms of the next layer above. On computationally compressing the PdH_2 layered structure, the layers come closer and after 15 GPa, a weak van der Waals (vdW) interaction comes into existence which is even manifested in the phonon dispersion curves by the occurrence of interlayer breathing modes (*vide infra*). As a consequence of the compression, the two layers are now held together by weak vdW forces. The H_{2b} atoms are roughly at intercalated positions between two Pd–H_{2a} monolayers. By 20 GPa, the H_{2b} atoms now become four fold coordinated with three Pd atoms in the layer beneath it and one Pd atom from the layer above it. Thus, the distance between the H_{2b} atoms and the three originally coordinated Pd atoms (0 GPa) increases from 1.87 to 1.95 Å while the distance between the H_{2b} atoms and the newly coordinated Pd atom in the layer above decreases from 3.30 to approximately 2 Å by 15 GPa. A more detailed explanation of the structures at ambient and compressed conditions have been reported in our other work [33]. The impact of the interlayer interactions via vdW bonding has been presented in this study with respect to electronic, vibrational and superconducting properties. The compressed structures have been treated with semi-empirical DFT-D2 corrections that incorporate the vdW corrections.

Electronic properties and fermi surface

At ambient pressure, $P6_3mc$ PdH_2 exhibits metallic properties. On compression, it tends to lose the metallicity. This is evident in Fig. 2, where we have shown the electronic band structures at 15 and 50 GPa. It is seen from Fig. 2a and b that both the electron and hole pockets due to the valence and conduction bands crossing the Fermi level tend to decrease considerably on the transition from low to high pressure. Thus, the metallic nature of PdH_2 diminishes. This trend of a metal or semi-metal towards becoming a non-metal on compression of layered structures has been established before as well [50]. This is also confirmed from the electronic density of states (DOS) shown in Fig. 2c and d for 15 and 40 GPa respectively. At pressures below 15 GPa, the 4d states of Pd contribute mostly to the total DOS around Fermi level. The H_{2a} 1s and H_{2b} 1s states have the same contribution to the DOS at around the Fermi level at ambient pressure and are degenerate. This is intuitive as both H_{2a} and H_{2b} are similarly bonded to the palladium atoms at ambient pressure. Applied pressure reduces the distance between the two layers of PdH_2. Interlayer interaction sets in and modifies the profile of the electronic properties. From Fig. 2c and d, it is clear that above the Fermi level, the H_{2b} 1s states contribute more to DOS than the H_{2a} 1s states. The first peak below the Fermi level shows that the H_{2a} and H_{2b} 1s states almost have the same contribution to the DOS. When pressure is applied, some small peaks for H 1s states can be found around Fermi level. At pressures below 15 GPa, the electrons are much more delocalized that those at higher pressures. We can see that with compression, there is hybridization of the Pd 4d and H 1s states. This increases the bonding between the layers of PdH_2, as a result of which the electrons become more localized, leading towards the loss of metallicity of the system.

In the K → Γ, Γ→M and H→K high symmetry paths (Fig. 2a and b), the flat and steep bands at the Fermi level are conspicuous. The occurrence of such flat and steep bands has been suggested as a characteristic that favours superconductivity [51–53]. The reason can be attributed as follows. Flat bands accommodate localized electrons which have very low or negligible velocities. These electrons according to conventional superconductivity are responsible for forming Cooper pairs. The delocalized electrons of the steep bands interact with the flat bands via phonons, causing a dynamic vibration of the Fermi level and contribute to the electron phonon coupling. Thus, studying the Fermi surface for Lifshitz transitions is of extreme importance, pertinent to phonon mediated superconductivity. On both sides of the Γ point (Fig. 2a and b), the flat bands correspond to van Hove singularities (*vHs*), which are manifested in the electronic Density of States (Fig. 2c and d) near the Fermi level in the form of discontinuous peaks. Since, at ambient pressure itself, the *vHs* occur close to the Fermi level, therefore, slight modulation in the

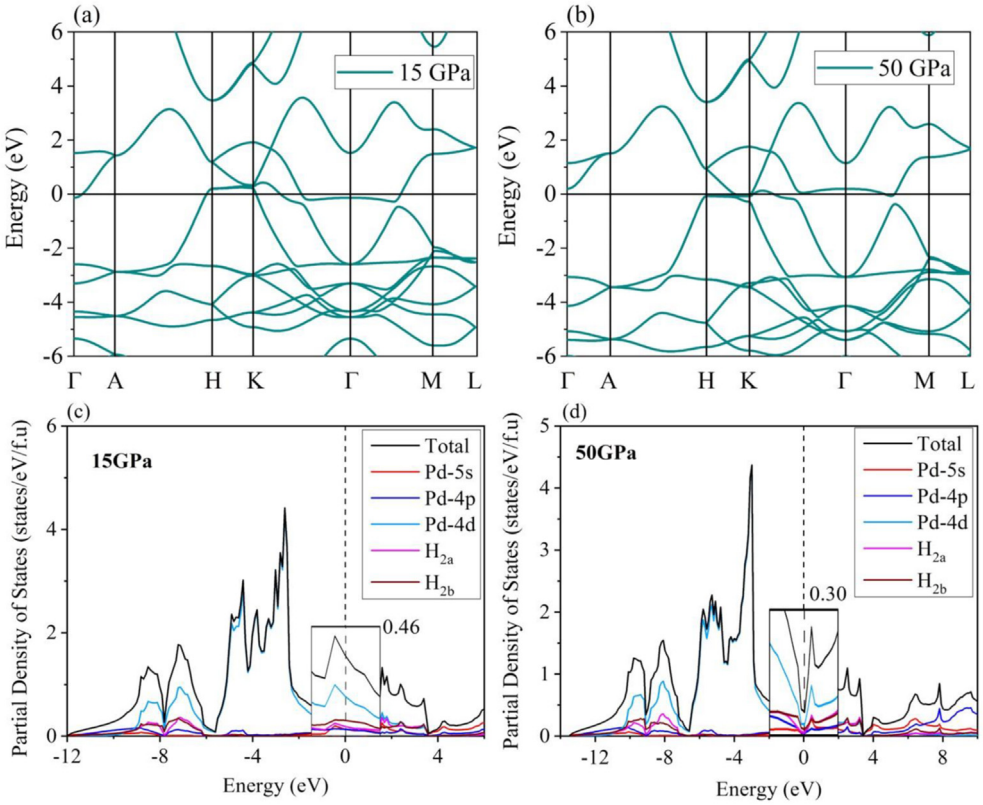

Fig. 2 – a-b) Electronic band structure and c-d) density of states of PdH_2 at 15 and 50 GPa respectively.

lattice can modify the position of the Fermi level. Between 30 and 40 GPa, the *vHs* is exactly at the Fermi level which has the potential to enhance the electron phonon coupling. The presence of such large *vHs* close to the Fermi level even at 0 GPa, can possibly be attributed as the reason for PdH_2 is an ambient pressure superconductor at a temperature below 24 K as well. In Fig. 3, we have shown the Fermi surfaces of the studied system at varying pressures. As the pressure is increased, there are noticeable changes in the area and topology of the Fermi surface. At 0 GPa, there is one pancake type pocket due to the electron pocket at the Γ point, and two hole type pockets at the K point. However, on compression, one of the hole pockets is significantly reduced in size and can't be visualized. On further compression to 40 GPa, both the hole and electron pockets decrease in magnitude (Fig. 3d), making the system transition towards non-metallicity. Such electronic instability also influences the superconductivity.

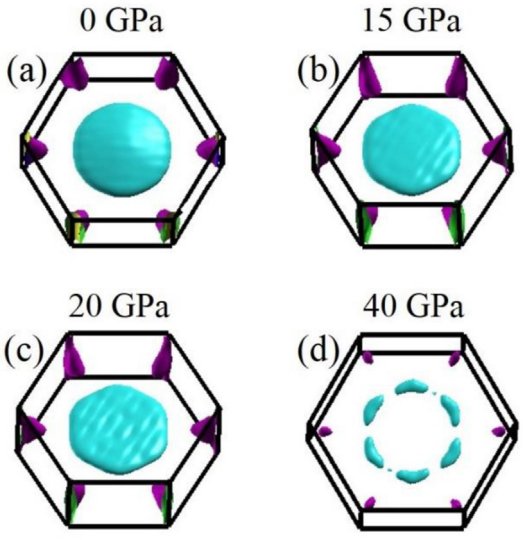

Fig. 3 – Fermi surface evolution with pressure of *P6₃mc* PdH_2 at a) 0, b) 15, c) 20 and d) 40 GPa.

The bonding environment of PdH_2 was investigated using the electron localization function (ELF) method [54]. Following a more intuitive approach, the ELF method characterizes the tendency of electron localization in crystals [55,56], with respect to a uniform electron gas of the same density. The ELF value is always positive and spans the range between 0 and 1. If the ELF value leans more towards 1 for a certain region, then there is a high tendency of electron pairing, such as cores, bonds, and lone pairs in that region. The ELF (Fig. 4) sheds some light on the bonding of PdH_2 at 0 and 15 GPa in the (100) and (001) atomic planes. The (100) plane reveals no interlayer bonding at 0 GPa. The distance between Pd–Pd, Pd–H_{2a}, and Pd–H_{2b} nearest neighbours are 4.415 Å, 1.873 Å, and 1.877 Å respectively at 0 GPa. At 15 GPa, the ELF in the (100) plane does not show electron localization between the layers either, although from our electronic and phonon dispersion (*vide infra*) we can infer interlayer interaction. Therefore, this interaction is not covalent. Thus, this further supports our claim that above 15 GPa, the layers are held together via weak vdW forces, due to which the electron localization between the layers is negligible. The distance between the Pd–Pd, the

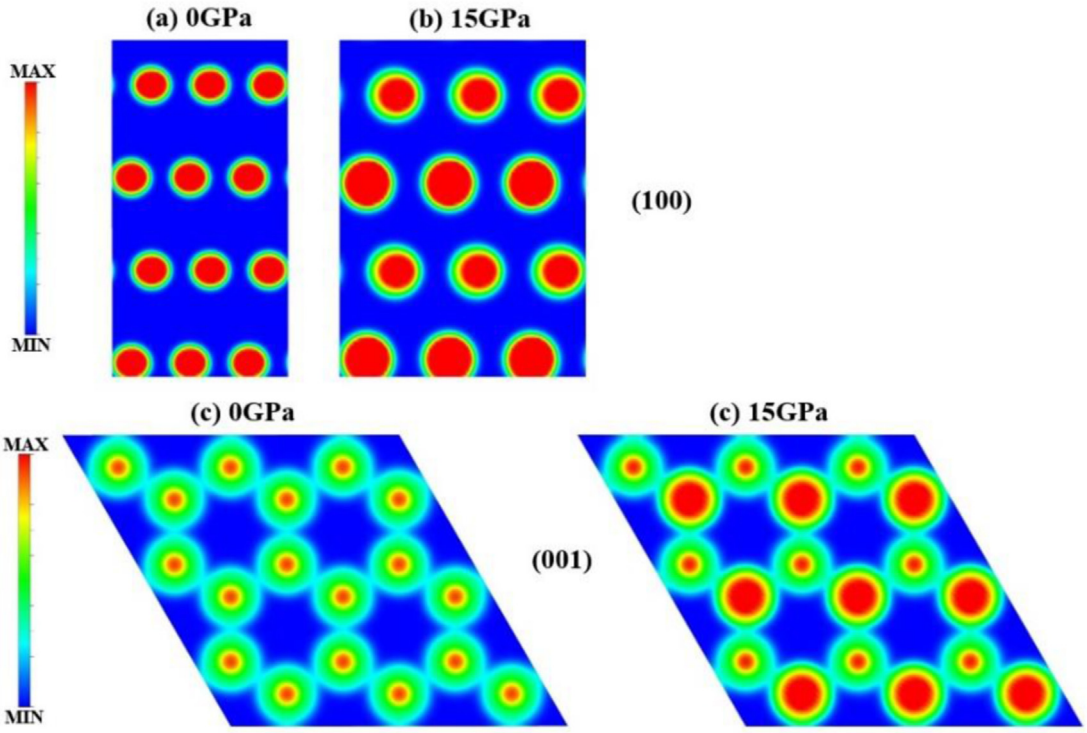

Fig. 4 – The electron localization function (ELF) in PdH_2. (a) ELF in the (100) atomic plane at 0 GPa, (b) ELF in the (100) atomic plane at 15 GPa, (c) ELF in the (001) atomic plane at 15 GPa, and (d) ELF in the (001) atomic plane at 15 GPa.

Pd–H_{2a}, and Pd–H_{2b} nearest neighbours at 15 GPa are 3.329 Å, 1.805 Å, and 1.940 Å, which are enough for the formation of vdW-bonded layered structure [57,58].

Dynamical stability

The dynamical stability of the $P6_3mc$ PdH_2 is confirmed from the phonon dispersion curves. Fig. 5a depicts the phonon dispersion curve of the monolayer PdH_2 at ambient pressure. It is evident that this $P6_3mc$ structure is dynamically stable at 0 GPa owing to the absence of imaginary frequencies. As can be seen from Fig. 5, the low frequency modes comprise of longitudinal (L), transverse (T) and out-of-plane (Z) acoustic modes, LA, TA and ZA respectively. For the monolayer, the optical branches (both transverse and longitudinal) have frequencies more than 19.55 THz at the gamma point. The implication of the distribution of these modes on superconductivity has been discussed later in this work.

Even these weakly interacting layered structures (above 15 GPa) are dynamically stable up to 60 GPa as shown in Fig. 5b-d. One of the most important consequences of the interlayer (IL) interactions is the rise of interlayer breathing modes. Due to the weak IL interaction, like other multilayered structures [59,60], besides the longitudinal and transverse optical modes, we also get out-of-plane optical modes represented by ZO. In bulk structures such as graphite or BN, these "organ pipe" or "breathing" modes cannot always be optically excited due to their optical inactivity, but they may show IR or Raman activity as pointed out by Michel and Verberck in multilayer graphene and BN [61,62]. These breathing modes are expected to exist in many 2D crystals and their layered morphologies. IL interactions are sensitive to the interlayer gaps and number of layers and prove to be very important for low-energy electronic and vibrational properties. In our system at 15 GPa, the ZO mode has a frequency of 3.34 THz at the Γ point. This ZO mode is a consequence of the Pd–H_{2a} bending vibration. Interestingly, although initially the frequency of the ZO mode at the Gamma point increases, but between 30 and 40 GPa, it plummets (Fig. 6). This paves the way for further studies on the trend of the magnitudes of the ZO modes for layered structures, in which the layers are held together by vdW forces and their impact on electronic and vibrational properties.

Phonon mediated superconductivity

At 15 GPa, after the monolayers are held weakly by London dispersion forces, two doubly degenerate phonon branches are seen in the dispersion curve above 30 THz (Fig. 5b). These correspond to the Pd–H stretch modes. The intermediate optical branches pertain to the Pd–H bent modes. The lattice vibrational breathing modes are responsible for the acoustic modes between 0 and 5 THz. Compared to the phonon dispersion profile at ambient pressure, at 15 GPa, the optical branches are much less densely spread. On further compressing the layers, the degeneracy of the high frequency stretch modes is seen to be broken by 20 GPa (Fig. 5c and d). Yet, the optical modes seem to be denser at 20 GPa than at 15 GPa. These vibrations (stretch and bent) all participate strongly in the electron-phonon interaction and shift the logarithmic average of the frequency to higher energy, yielding a higher T_c. Thus, an increase in T_c is seen between 15 and 20 GPa as the logarithmic average of the frequency

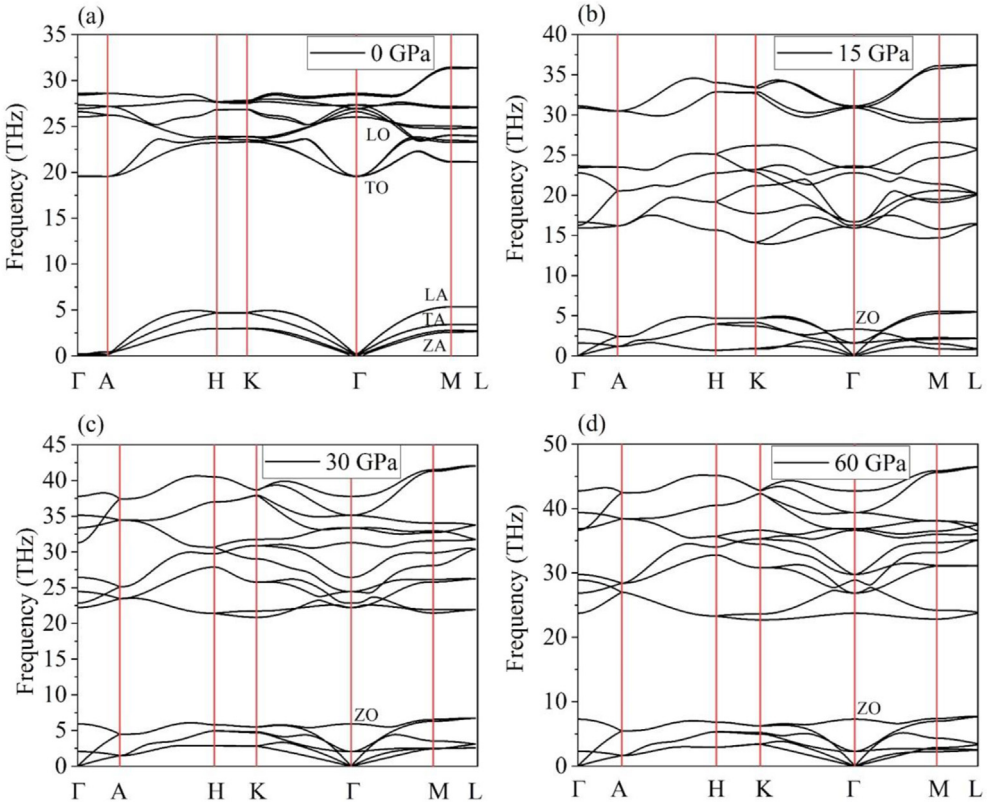

Fig. 5 – Phonon dispersion curves of $P6_3mc$ PdH2 at 1) 0 b) 15 c) 20 and d) 40 GPa.

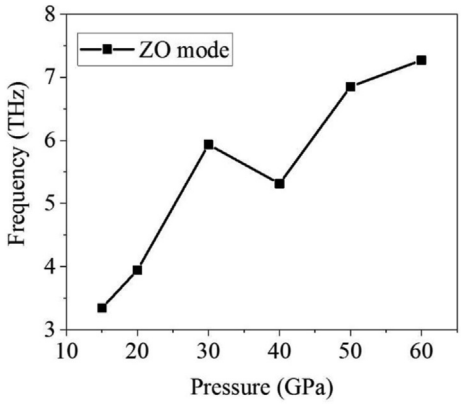

Fig. 6 – Out–of-plane ZO mode at the Gamma point as a function of pressure.

increases. However, remarkably, beyond 20 GPa, the trend reverses. Now, both the stretch and bent modes harden on being compressed and become closer, thus enhancing the proper mixing needed for a considerable electron phonon coupling coefficient. But besides the logarithmic average being high, a sensitive combination of it along with λ is required for high T_c, consistent with the theory put forward by Tanaka et al. [63] which shows that mixing of phonon bands is a key ingredient for higher T_c. Although the electron phonon coupling (EPC) strength λ may be calculated at a deeper level of theory, in first principles calculations for hydrides, T_c is often estimated using several approximations, such as the lack of first principles treatment of Coulombic pseudopotential (μe). Therefore, the theoretical critical temperatures are calculated only for a consistency check and to see the trends, rather than the unequivocal confirmation of the experimental results. According to the Migdal-Eliashberg theory [64,65] the electron phonon coupling (EPC) parameter λ obtained by integrating the electron-phonon spectral function $\alpha^2F(\omega)$,

$$\lambda = 2\int_0^{\infty} \frac{\alpha^2 F(\omega)}{\omega} d\omega. \quad (1)$$

In strong coupling region, the T_c can be estimated using the Allen-Dynes modification of the McMillan equation [66],

$$T_c = \frac{\omega_{log}}{1.2} \exp\left[-\frac{1.04(1+\lambda)}{\lambda - \mu^*(1+0.62\lambda)}\right], \quad (2)$$

where ω_{log} is the logarithmic average of phonon frequencies and μ^* is the Coulomb pseudopotential representing the screened Coulombic repulsion. Here, we have calculated the λ, T_c and ω_{log} for all the studied pressure points between 0 and 60 GPa. The value of the Coulomb pseudopotential was set to be 0.13, which is a standard value as can be seen in other calculations pertinent to hydrides. As can be seen from Fig. 6b, the trends of the λ, T_c and ω_{log} confirm our explanation of the superconducting properties on the basis of the phonons as discussed above.

The logarithmic average of the frequency initially decreases between 0 and 15 GPa but then rises sharply between 15 and 20 GPa before falling again. At ambient pressure, the PdH_2 structure is calculated to have a critical temperature of 24 K. As

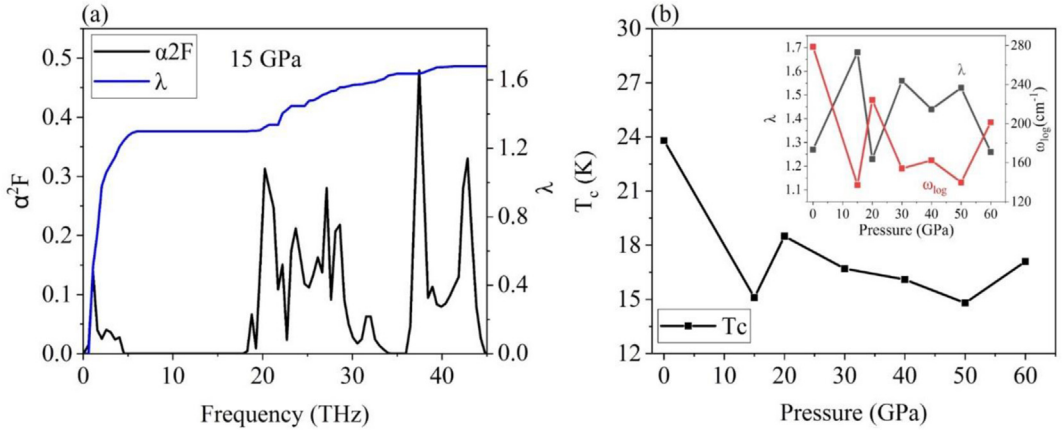

Fig. 7 – a) Eliashberg spectral function and EPC at 15 GPa, and b) T_c vs pressure.

mentioned previously, at 15 GPa, the sudden appearance of the out of plane breathing mode (ZO), and well separated phonon bands drops the ω_{log}, leading to a decreased T_c value of 15 K. The reverse trend is obtained between 15 and 20 GPa where the T_c increases to a value to 19 K. In this interval the effect of the ω_{log} weighs down the effect of the λ. The sharp increase in the EPC at 15 GPa can be explained as a consequence of the phase transition at 15 GPa. Phase transitions are characterized by lattice instabilities, which enhance the electron phonon coupling. Hence, the increment of the λ is justified. Beyond 20 GPa up to 60 GPa, the weakly interacting layered structure maintains the same structural morphology albeit with lesser interlayer gaps. The dominant nature of the ω_{log} once again assists in monotonically decreasing the T_c above 20 GPa. Although, there is a fluctuation in the values of the logarithmic average and EPC, but the T_c keeps decreasing with pressure beyond 20 GPa, before it starts to increase once again after 50 GPa. In the inset of Fig. 7b, both the ω_{log} and λ have oscillating values rather than monotonic. So, possibly there are several competing factors which eventually contribute to the λ and ω_{log}. Therefore, taking the idea of conventional superconducting hydrides one step ahead, it is probably safe to infer that the superconducting properties that we obtained from the calculations, specifically beyond 15 GPa, are dependent on the van Hove singularity around the Fermi energy, the mixing profile of the optical modes as well and the value of ZO interlayer breathing mode frequency at the gamma point. A sensitive combination of these three factors determines the T_c for the PdH_2 system that we have studuied. Breathing modes may lead to charge fluctuation [67]. These out-of-plane transverse vibrations contribute to electron phonon coupling near the Fermi level. On computationally imparting more pressure to the layered structure, the interlayer gap decreases, increasing the force constant and eventually the frequency of the ZO modes. This can be seen in Fig. 6. On comparing the inset of Fig. 7b with Fig. 6, one can notice that the λ drops after 30 GPa which is consistent with the drop in the frequency of the ZO mode too after 30 GPa. The close correlation between the frequency of the ZO mode and the λ can also be inferred from Fig. 6a. There is a sudden increase in the λ below 5 THz, which strengthens our conclusion that the ZO modes contribute a significant percentage to the electron phonon coupling. Beyond 50 GPa, the overall hardening of the phonons inhibits electron phonon coupling, and moreover the *vHs* has moved further up away from the Fermi level, thereby rendering the ω_{log} as the main contributor to T_c. The intermediate pressure range of this study (30–50 GPa) is of particular interest as both effect of the *vHs* and ZO mode become quite noticeably conflicting.

Conclusion

In summary, we have studied the electronic, vibrational and superconducting properties of the predicted $P6_3mc$ layered hexagonal structure of PdH_2. This layered van der Waals structure has been shown to exhibit an uncommon combination of several different phenomena. From the electronic properties, we have found van Hove singularity around the Fermi level. This *vHs* is dynamic with compression and moves from below the Fermi level to above it on compression between 30 and 40 GPa. The vibrational properties also unravel an interesting phenomenon in the form of an out-of-plane interlayer breathing (ZO) mode above 15 GPa. This is a signature to the fact that the layers are held together by weakly interacting van der Waals forces. With a decrease in the unit cell volume, the frequency of this ZO mode increases except for in a small pressure range between 30 and 40 GPa once again. Therefore, the presence of both *vHs* and ZO mode is capable of tuning the superconducting properties considerably. Following the claims made in previous studies regarding palladium hydrides to be ambient pressure superconductors [29,30], we calculated the superconducting properties of the studied system at various pressure points. Indeed, it is a superconductor at 0 GPa with a T_c of 24 K. As per our intuition about the evolution of superconducting properties with pressure with respect to *vHs* and ZO mode, we found from our calculations that the ZO mode contributes significantly to the λ. In the 30–40 GPa pressure range, the decrement in the frequency of the ZO mode is calculated to be more dominant than the *vHs* crossing the Fermi level while describing the superconductivity. Therefore, unlike most other studied hydride systems, for this layered structure of PdH_2, the presence of ZO mode and *vHs* also play crucial roles in determining the superconductivity. Our work paves the way for further studies to be done on

superconducting properties of layered structures showing unique vibrational properties owing to van der Waals interactions.

Declaration of competing interest

The authors declare that they have no known competing financial interests or personal relationships that could have appeared to influence the work reported in this paper.

Acknowledgements

This research project is supported by the Second Century Fund (C2F), Chulalongkorn University. This project is funded by National Research Council of Thailand (NRCT): (NRCT5-RSA63001-04). This research is partially funded by Chulalongkorn University; Grant for Research. This Research is funded by Thailand Science research and Innovation Fund Chulalongkorn University (IND66230002). We also gratefully acknowledge computational resources from the Swedish National Infrastructure for Computing SNIC (2021/1–42) and HPC2N. R.A. and W.L. thank the Swedish Research Council (VR-2016- 06014 & VR-2020-04410), Sweden (2021–00665) for financial support.

REFERENCES

[1] Ashcroft NW. Metallic hydrogen: a high-temperature superconductor? Phys Rev Lett 1968;21:1748. https://doi.org/10.1103/PhysRevLett.21.1748.
[2] Ashcroft NW. Hydrogen dominant metallic alloys: high temperature superconductors? Phys Rev Lett 2004;92:187002. https://doi.org/10.1103/PhysRevLett.92.187002.
[3] Bardeen J, Cooper LN, Schrieffer JR. Theory of superconductivity. Phys Rev 1957;108:1175. https://doi.org/10.1103/PhysRev.108.1175.
[4] Sukmas W, Tsuppayakorn-aek P, Pluengphon P, Clark SJ, Ahuja R, Bovornratanaraks T, Luo W. First-principles calculations on superconductivity and H-diffusion kinetics in Mg–B–H phases under pressures. https://doi.org/10.1016/j.ijhydene.2022.10.232; 2022.
[5] Eremets MI, Trojan IA, Medvedev SA, Tse JS, Yao Y. Superconductivity in hydrogen dominant materials: silane. Science 2008;319:1506. https://doi.org/10.1126/science.1153282.
[6] Chen XJ, Wang JL, Struzhkin VV, Mao HK, Hemley RJ, Lin HQ. Superconducting behavior in compressed solid SiH4 with a layered structur. Phys Rev Lett 2008;101:077002. https://doi.org/10.1103/PhysRevLett.101.077002.
[7] Strobel TA, Goncharov AF, Seagle CT, Liu Z, Somayazulu M, Struzhkin VV, Hemley RJ. High-pressure study of silane to 150 GPa. Phys Rev B 2011;83:144102. https://doi.org/10.1103/PhysRevB.83.144102.
[8] Shamp A, Zurek E. Superconducting high-pressure phases composed of hydrogen and iodine. J Phys Chem Lett 2015;6:4067. https://doi.org/10.1021/acs.jpclett.5b01839.
[9] Zurek E, Hoffmann R, Ashcroft NW, Oganov AR, Lyakhov AO. A little bit of lithium does a lot for hydrogen. Proc Natl Acad Sci USA 2009;106:17640. https://doi.org/10.1073/pnas.0908262106.
[10] Drozdov AP, Eremets MI, Troyan IA, Ksenofontov V, Shylin SI. Conventional superconductivity at 203 kelvin at high pressures in the sulfur hydride system. Nature 2015;525:73. https://doi.org/10.1038/nature14964.
[11] Majumdar A, Tse JS, Yao Y. Modulated structure calculated for superconducting hydrogen sulfide. Angew Chem, Int Ed Engl 2017;56:11390. https://doi.org/10.1002/ange.201704364.
[12] Pépin CM, Geneste G, Dewaele A, Mezouar M, Loubeyre P. Synthesis of FeH5: a layered structure with atomic hydrogen slabs. Science 2017;357:382. https://doi.org/10.1126/science.aan0961.
[13] Majumdar A, Tse JS, Wu M, Yao Y. Superconductivity in FeH5. Phys Rev B 2017;96:201107. https://doi.org/10.1103/PhysRevB.96.201107.
[14] Majumdar A, Tse JS, Yao Y. Mechanism for the structural transformation to the modulated superconducting phase of compressed hydrogen sulfide. Sci Rep 2019;9:5023. https://doi.org/10.1038/s41598-019-41607-1.
[15] Feng J, Grochala W, Jaroń T, Hoffmann R, Bergara A, Ashcroft and NW. Structures and potential superconductivity in SiH4 at high pressure: en route to "metallic hydrogen". Phys Rev Lett 2006;96:017006. https://doi.org/10.1103/PhysRevLett.96.017006.
[16] Tse JS, Yao Y, Tanaka K. Novel superconductivity in metallic SnH4 under high pressure. Phys Rev Lett 2007;98:117004. https://doi.org/10.1103/PhysRevLett.98.117004.
[17] Wang H, Tse JS, Tanaka K, Iitaka T, Ma Y. Superconductive sodalite-like clathrate calcium hydride at high pressures. Proc Natl Acad Sci USA 2012;109:6463. https://doi.org/10.1073/pnas.1118168109.
[18] Gao G, Oganov AR, Bergara A, Martinez-Canales M, Cui T, Iitaka T, Ma Y, Zou G. Superconducting high pressure phase of germane. Phys Rev Lett 2008;101:107002. https://doi.org/10.1103/PhysRevLett.101.107002.
[19] Li Y, Gao G, Xie Y, Ma Y, Cui T, Zou G. Superconductivity at ~100 K in dense SiH4(H2)2 predicted by first principles. Proc Natl Acad Sci USA 2010;107:15708. https://doi.org/10.1073/pnas.1007354107.
[20] Kim DY, Scheicher RH, Ahuja R. Predicted high-temperature superconducting state in the hydrogen-dense transition-metal hydride YH3 at 40 K and 17.7 GPaPhys. Rev Let 2009;103:077002. https://doi.org/10.1103/PhysRevLett.103.077002.
[21] Kruglov IA, Kvashnin AG, Goncharov AF, Oganov AR, Lobanov SS, Holtgrewe N, Jiang S, Prakapenka VB, Greenberg E, Yanilkin AV. Uranium polyhydrides at moderate pressures: prediction, synthesis, and expected superconductivity. Sci Adv 2018;4:eaat9776. https://doi.org/10.1126/sciadv.aat9776.
[22] Semenok DV, Kvashnin AG, Kruglov IA, Oganov AR. Actinium hydrides AcH10, AcH12, and AcH16 as high-temperature conventional superconductors. J Phys Chem Lett 2018;9:1920. https://doi.org/10.1021/acs.jpclett.8b00615.
[23] Liu H, Naumov II, Hoffmann R, Ashcroft NW. Hemley RJ Potential high-Tc superconducting lanthanum and yttrium hydrides at high pressure. Proc Natl Acad Sci USA 2017;114:6990. https://doi.org/10.1073/pnas.1704505114.
[24] Somayazulu M, Ahart M, Mishra AK, Geballe ZM, Baldini M, Meng Y, Struzhkin VV, Hemley RJ. Evidence for superconductivity above 260 K in lanthanum superhydride at megabar pressures. Phys Rev Lett 2019;122:027001. https://doi.org/10.1103/PhysRevLett.122.027001.
[25] Somayazulu M, Dera P, Smith J, Hemley RJ. Structure and stability of solid Xe(H2)n. J Chem Phys 2015;142:104503. https://doi.org/10.1063/1.4908265.
[26] Somayazulu M, Dera P, Goncharov AF, Gramsch SA, Liermann P, Yang W, Liu Z, Mao HK, Hemley RJ. Pressure-induced bonding and compound formation in

xenon–hydrogen solids. Nat Chem 2009;2:50. https://doi.org/10.1038/nchem.445.
[27] Santra B, Klimeš J, Alfè D, Tkatchenko A, Slater B, Michaelides A, Car R, Scheffler M. Hydrogen bonds and van der Waals forces in ice at ambient and high pressures. Phys Rev Lett 2011;107:185701. https://doi.org/10.1103/PhysRevLett.107.185701.
[28] Strobel TA, Somayazulu M, Hemley RJ. Novel pressure-induced interactions in silane-hydrogen. Phys Rev Lett 2009;103:065701. https://doi.org/10.1103/PhysRevLett.103.065701.
[29] Stritzker B, Buckel. Superconductivity in the palladium-hydrogen and the palladium-deuterium systems. W. Zeitschrift Für Phys. 1972;257:1. https://doi.org/10.1007/BF01398191.
[30] Schirber JE, Northrup Jr CJM. Concentration dependence of the superconducting transition temperature in PdHx and PdDx. Phys Rev B 1974;10:3818. https://doi.org/10.1103/PhysRevB.10.3818.
[31] Skoskiewicz T. Superconductivity in the palladium-hydrogen and palladium-nickel-hydrogen systems. Phys Status Solidi 1972;11:K123. https://doi.org/10.1002/pssa.2210110253.
[32] Syed HM, Gould TJ, Webb CJ, Gray EM. Superconductivity in palladium hydride and deuteride at 52-61 kelvin. Arxiv 2016. https://doi.org/10.48550/arXiv.1608.01774. 1608.01774:1.
[33] Liu Z, Ahuja R, Li H, Luo W. Mechanical and electronic properties of van der Waals layered hcp PdH2. Sci Rep 2020;10:8037. https://doi.org/10.1038/s41598-020-61385-5.
[34] Pickard CJ, Needs RJ. High-pressure phases of silane. Phys Rev Lett 2006;97:0455041. https://doi.org/10.1103/PhysRevLett.97.045504.
[35] Pickard CJ, Needs RJ. Ab initio random structure searching. J Phys Condens Matter 2011;23:053201. https://doi.org/10.1088/0953-8984/23/5/053201.
[36] Ichinokura S, Sugawara K, Takayama A, Takahashi T, Hasegawa S. Superconducting calcium-intercalated bilayer graphene. ACS Nano 2016;10:2761. https://doi.org/10.1021/acsnano.5b07848.
[37] Xue M, Chen G, Yang H, Zhu Y, Wang D, He J, Cao T. Superconductivity in potassium-doped few-layer graphene. J Am Chem Soc 2012;134:6536. https://doi.org/10.1021/ja3003217.
[38] Kresse G, Hafner J. Ab initio molecular dynamics for liquid metals. Phys Rev B 1993;47:558. https://doi.org/10.1103/PhysRevB.47.558.
[39] Kresse G, Furthmüller and J. Efficient iterative schemes for ab initio total-energy calculations using a plane-wave basis set. Phys Rev B 1996;54:11169. https://doi.org/10.1103/PhysRevB.54.11169.
[40] Giannozzi P, Baroni S, Bonini N, Calandra M, Car R, Cavazzoni C, Ceresoli D, Chiarotti GL, Cococcioni M, Dabo I, Corso AD, Gironcoli SD, Fabris S, Fratesi G, Gebauer R, Gerstmann U, Gougoussis C, Kokalj A, Lazzeri M, Martin-Samos L, Marzari N, Mauri F, Mazzarello R, Paolini S, Pasquarello A, Paulatto L, Sbraccia C, Scandolo S, Sclauzero G, Seitsonen AP, Smogunov A, Umari P, Wentzcovitch RM. Quantum ESPRESSO: a modular and open-source software project for quantum simulations of materials. J Phys Condens Matter 2009;21:3955022. https://doi.org/10.1088/0953-8984/21/39/395502.
[41] Blochl PE. Projector augmented-wave method. Phys Rev B 1994;50:17953. https://doi.org/10.1103/PhysRevB.50.17953.
[42] Kresse G, Joubert D. From ultrasoft pseudopotentials to the projector augmented-wave method. Phys Rev B 1999;59:1758. https://doi.org/10.1103/PhysRevB.59.1758.
[43] Perdew JP, Burke K, Ernzerhof M. Generalized gradient approximation made simple. Phys Rev Lett 1996;77:3865. https://doi.org/10.1103/PhysRevLett.77.3865.
[44] Monkhorst HJ, Pack JD. Special points for Brillouin-zone integrations. Phys Rev B 1976;13:5188. https://doi.org/10.1103/PhysRevB.13.5188.
[45] Togo A, Chaput L, Tanaka I, Hug G. First-principles phonon calculations of thermal expansion in Ti3SiC2, Ti3AlC2, and Ti3GeC2. Phys Rev B 2010;81:174301. https://doi.org/10.1103/PhysRevB.81.174301.
[46] Togo A, Tanaka I. First principles phonon calculations in materials science. Scripta Mater 2015;108:1. https://doi.org/10.1016/j.scriptamat.2015.07.021.
[47] Grimme S. Semiempirical GGA-type density functional constructed with a long-range dispersion correction. J Comput Chem 2006;27:1777. https://doi.org/10.1002/jcc.20495.
[48] Luo D, Li J, Zhang Y, Song Y, Chen H. Electronic structure and hydrogen storage properties of Li–decorated single layer blue phosphorus. Int. J. Hydrog. 2018;43:8415. https://doi.org/10.1016/j.ijhydene.2018.03.115.
[49] Zhou H, Zhang W, Li L, Sun F, Hong A. Doping engineering: highly improving hydrogen evolution reaction performance of monolayer SnSe. Int. J. Hydrog. 2021;46:37907. https://doi.org/10.1016/j.ijhydene.2021.09.027.
[50] Kou L, Hu F, Yan B, Frauenheim T, Chen C. Opening a band gap without breaking lattice symmetry: a new route toward robust graphene-based nanoelectronics. Nanoscale 2014;6:7474. https://doi.org/10.1039/C4NR01102C.
[51] Simon A. Superconductivity and chemistry. Angew Chem 1997:361788. https://doi.org/10.1002/anie.199717881.
[52] Deng S, Simon A, Köhler J. Chemical bonding variations and Electron–Phonon interactions. J Am Chem Soc 2002;1214:10712. https://doi.org/10.1021/ja011815q.
[53] Deng S, Simon A, Köhler J. A "flat/steep band" scenario in momentum space. J Supercond 2004;17:227. https://doi.org/10.1023/B:JOSC.0000021247.78801.78.
[54] Becke AD, Edgecombe KE. A simple measure of electron localization in atomic and molecular systems. https://doi.org/10.1063/1.458517; 1990.
[55] Pluengphon P, Tsuppayakorn-aek P, Sukmas W, Inceesungvorn B, Bovornratanaraks T. Dynamical stabilization and H-vacancy diffusion kinetics of lightweight complex hydrides: ab initio study for hydrogen storage improvement. https://doi.org/10.1016/j.ijhydene.2021.04.070; 2021.
[56] Liu G, Li J, Dong C, Wu L, Liang D, Caob H, Lu P. Hydrogen evolution reaction on in-plane platinum and palladium dichalcogenides via single-atom doping. https://doi.org/10.1016/j.ijhydene.2021.02.206; 2021.
[57] Björkman T, Gulans A, Krasheninnikov AV, Nieminen RM. van der Waals bonding in layered compounds from advanced density-functional first-principles calculations. Phys Rev Lett 2012;108:235502. https://doi.org/10.1103/PhysRevLett.108.235502.
[58] Thonhauser T, Cooper VR, Li S, Puzder A, Hyldgaard P, Langreth DC. Van der Waals density functional: self-consistent potential and the nature of the van der Waals bond. Phys Rev B 2007;76:125112. https://doi.org/10.1103/PhysRevB.76.125112.
[59] Yanagisawa H, Tanaka T, Ishida Y, Matsue M, Rokuta E, Otani S, Oshima C. Phonon dispersion curves of a BC3 honeycomb epitaxial sheet. Phys Rev Lett 2004;93:177003. https://doi.org/10.1103/PhysRevLett.93.177003.
[60] Yan JA, Ruan WY, Chou MY. Phonon dispersions and vibrational properties of monolayer, bilayer, and trilayer graphene: density-functional perturbation theory. Phys Rev B 2008;77:125401. https://doi.org/10.1103/PhysRevB.77.125401.
[61] Michel KH, Verberck B. Theoretical phonon dispersions in monolayers and multilayers of hexagonal boron-nitride.

Phys. Status Solidi Basic Res. 2009;246:2802. https://doi.org/10.1002/pssb.200982307.
[62] Michel KH, Verberck B. Phonon dispersions and piezoelectricity in bulk and multilayers of hexagonal boron nitride. Phys Rev B 2011;83:115328. https://doi.org/10.1103/PhysRevB.83.115328.
[63] Tanaka K, Tse JS, Liu H. Electron-phonon coupling mechanisms for hydrogen-rich metals at high pressure. Phys Rev B 2017;96:100502. https://doi.org/10.1103/PhysRevB.96.100502.
[64] Migdal AB. Interaction between electrons and lattice vibrations in a normal metal. Sov Phys JETP 1958;34:1438.
[65] Éliashberg GM. Interactions between electrons and lattice vibrations in a superconductor. Sov Phys JETP 1960;11:969.
[66] Allen PB, Dynes RC. Transition temperature of strong-coupled superconductors reanalyzed. Phys Rev B 1975;12:905. https://doi.org/10.1103/PhysRevB.12.905.
[67] Mattheiss LF. Electronic band properties and superconductivity in $La_{2-y}X_yCuO_4$. Phys Rev Lett 1987;58:1028. https://doi.org/10.1103/PhysRevLett.58.1028.